

DETERMINATION OF THE DRIFT VELOCITY AND THE VOID FRACTION FOR THE BUBBLE- AND PLUG-FLOW REGIMES DURING THE FLOW BOILING OF WATER AT ELEVATED PRESSURES

H. C. ÜNAL

Central Technical Institute TNO, P.O. Box 342, Apeldoorn, The Netherlands

(Received 20 June 1977)

Abstract—Drift velocity was measured at elevated pressures with high-speed photography for the bubble and plug-flow regimes in a 10 m long sodium heated steam generator tube of 0.008 m I.D. The operating conditions for the test were: pressure: 4.3–18 MN/m²; mass velocity: 51–107 kg/m² s; outlet subcooling: 0–1.3 K; void fraction: 0.0008–0.26. The data were correlated with a dimensionless equation. For the operating conditions considered, the drift velocity does not significantly change. In order to determine the void fraction for a wide range of conditions in small-diameter circular tubes, annuli and rectangular channels, the correlation of the author was slightly modified. The correlation applies to both high and low mass velocities. The drag coefficient for the motion of a bubble (or a plug) in a turbulent water stream is shown to be a function of bubble (or plug) Reynolds number and geometry. During the experiments, for the pressure range from 4.3 MN/m² up to 14.2 MN/m², the flow pattern in the test tube changed periodically from bubble flow to plug flow. The frequency of the observed instabilities varied between 10 and 50 Hz. The cause of this type of instability is anticipated to be the suppression of the bubble growth.

NOMENCLATURE

A ,	cross-sectional area [m ²];
C ,	distribution parameter;
C_d ,	drag coefficient;
D ,	equivalent-bubble or -plug diameter [m];
d ,	tube diameter or hydraulic diameter [m];
G ,	mass velocity [kg/m ² s];
g ,	acceleration of gravity [m/s ²];
J ,	volume flux density [m/s];
\bar{J} ,	average volumetric flux density of a two-phase mixture [m/s];
k ,	number of bubbles in a sample;
m ,	total number of plugs and/or bubbles in the sapphire test section;
n ,	number of axial positions;
P ,	pressure [N/m ²];
P_r ,	reduced pressure (i.e. pressure divided by critical pressure);
Q ,	volumetric flow rate [m ³ /s];
q ,	heat flux [W/m ²];
R ,	volume of the sapphire test section [m ³];
Re ,	Reynolds number;
Δt ,	subcooling, i.e. difference between saturation temperature and bulk liquid temperature [K];
U ,	weighted mean velocity of the vapour phase [m/s];
u ,	difference between the time-averaged bubble or plug velocity and the local liquid velocity [m/s];
V ,	instantaneous bubble or plug velocity [m/s];
\bar{V} ,	time-averaged bubble or plug velocity [m/s];
V_d ,	weighted mean drift velocity [m/s];

\bar{V}_d ,	drift velocity, average over cross-section [m/s];
V_v ,	velocity of vapour phase [m/s];
\bar{V}_v ,	velocity of vapour phase, average over cross-section [m/s];
v_d ,	drift velocity [m/s];
X ,	steam quality;
Y ,	variable.

Greek symbols

α ,	void fraction;
$\bar{\alpha}$,	void fraction, average over cross-section;
β ,	vapour volumetric rate ratio;
μ ,	dynamic viscosity [kg/m s];
ρ ,	density [kg/m ³];
σ ,	surface tension [N/m].

Subscripts

L ,	refers to liquid phase;
M ,	refers to measured value;
P ,	refers to predicted value;
v ,	refers to vapour phase.

INTRODUCTION

DRIFT velocity is the difference between the velocity of one of the phases and the average velocity of the mixture of the vapour and liquid phases during the flow boiling of a liquid [1]. This velocity has to be known for the accurate determination of the void fraction, which is of importance to predict pressure drop and two-phase flow instabilities in steam generators and liquid-cooled reactors.

No literature exists on the adequate determination of the drift velocity for bubble- and plug-flow regimes during the flow boiling of water at elevated pressures.

Many investigators have reported data on the motion of gas bubbles in liquids (for references see [2-4]). Most of their studies deal with the motion of individual air bubbles in a stagnant water and in a turbulent water stream. However, no scaling-law has yet been established between the motion of individual gas bubbles and the motion of the flow boiling bubbles. The latter form, in fact, a population consisting of many different sizes of bubbles with different velocities. For the velocity of the vapour phase in the bubble- (or plug-) flow regime, the velocity of the whole bubble (or plug) population has to be considered. A statistical approach is therefore required to determine the velocity of a bubble (or plug) population.

A velocity field which is useful for characterizing the flow of a two-phase mixture is given by Zuber and Findlay [1]

$$\bar{V}_v = \bar{J} + \bar{V}_d \quad (1)$$

where

$$\bar{J} = (Q_L + Q_v)/A = G/\rho_v [X + (1-X)(\rho_v/\rho_L)] \quad (2)$$

Weighting every term in equation (1) with void fraction and dividing by \bar{J} , they obtained

$$U/\bar{J} = C + V_d/\bar{J} \quad (3)$$

or

$$\beta/\bar{\alpha} = C + V_d/\bar{J} \quad (4)$$

where

$$\beta = Q_v/(Q_v + Q_L) = X/\rho_v [X/\rho_v + (1-X)/\rho_L]^{-1} \quad (5)$$

$$U = \frac{\langle V_v \alpha \rangle}{\langle \alpha \rangle} \quad (6)$$

$$C = \frac{\langle \alpha J \rangle}{\langle \alpha \rangle \langle J \rangle} \quad (7)$$

$$V_d = \frac{\langle v_d \alpha \rangle}{\langle \alpha \rangle} \quad (8)$$

$$v_d = V_c - J \quad (9)$$

The $\langle \rangle$'s denote averages over the cross-section defined by equation

$$\langle Y \rangle = \frac{\int Y dA}{A} \quad (10)$$

For the diabatic and adiabatic flow of steam-water mixtures in small-diameter vertical channels, it is reported in [5,6]

$$C = 1.13 \quad (11)$$

$$V_d = 1.18 [\sigma g (\rho_L - \rho_v) / \rho_L^2]^{0.25} \quad (12)$$

and in [7]

$$C = 1.00 \quad (13)$$

$$V_d = 0.36(1 - P_r)^{0.9} \quad (14)$$

For the data discussed in [5-7], $V_d/\bar{J} \ll 1$. It follows from equation (4) that the weighted mean drift velocity (which will be termed simply "drift velocity" further

on) given by equations (12) and (14) can not be accurate since $C \geq 1$, as already indicated in [7].

In order to determine void fraction properly with equation (3) or (4) for the condition $V_d/\bar{J} \geq 1$, i.e. for low mass velocities, the accurate value of the drift velocity has to be known.

In the present work for the determination of the drift velocity, a modified version of equation (1) is used. For low steam qualities and void fractions the average volumetric flux density of the vapour-liquid mixture is practically equal to that of the liquid. In such cases it is sufficient for the determination of the drift velocity to measure the weighted mean velocity of the vapour phase (i.e. the velocity of the centre of gravity of the vapour phase), and equation (1) then reduces to

$$U = \bar{J} + V_d \quad (15)$$

and \bar{J} in the above equation is a known function of the operating conditions [see equation (2)]. However, as can be seen from equation (15), for the accurate determination of the drift velocity its magnitude has to be in the same order of magnitude as \bar{J} .

This paper presents data for the drift velocity obtained with the condition $V_d/\bar{J} = 0.75-2.22$. U , the weighted mean velocity of the vapour phase (or velocity of the centre of gravity of the vapour phase) was measured with high-speed photography. The aforesaid data have been used to modify equations (13) and (14) to predict the void fraction both for low and high mass velocities. Data for the drag coefficient for the motion of flow boiling bubbles and plugs, and data for the flow pattern instabilities have also been presented.

TEST SET-UP, PROCEDURE AND CONDITIONS

The photographic test section was an adiabatic, square sapphire channel of $0.0071 \times 0.0071 \times 0.02$ m. The wall thickness of the channel was 0.003 m. This test section was mounted at the end of a 10 m long, straight vertical sodium heated steam generator test tube of 0.008 m I.D. The test tube was installed in a heat transfer loop, which is described in [7]. A 0.02 m long transition piece was mounted between the sapphire channel and the test tube. The cross-sectional area along this piece was practically equal to the cross-sectional area of the test tube and of the sapphire channel.

The pictures of subcooled nucleate flow boiling were taken through the sapphire channel with a high-speed rotating prism camera (Hycam model, 120 m) at a frequency of 10 000 frames/s for the following range of operating conditions:

$$P, 4.3-18 \text{ MN/m}^2;$$

$$G, 51-107 \text{ kg/m}^2 \text{ s};$$

$$\Delta t, 0-1.3 \text{ K};$$

$$\alpha, 0.08-26\%.$$

The operating conditions are also summarized in Table 1.

When making the experiments, it took half an hour to reach steady-state conditions, after which photographs were taken.

Table 1. Operating conditions for the tests

P (MN/m ²)	G (kg/m ² s)	$\bar{\alpha}$ (%)	D (mm)	U (m/s)	\bar{V} (m/s)
10.1	93.6	14.6	3.33–5.73	0.345	0.32–0.35
14.2	74.5	26	1.10–5.90	0.353	0.29–0.355
4.3	59.5	2.5	3.19–3.56	0.24–0.25	0.24–0.25
7.3	62.5–87.6	0.08–4.6	1.08–3.67	0.25–0.34	0.25–0.34
10.1	61.3–73.7	2.7–4.4	1.23–3.87	0.229–0.295	0.22–0.33
12.2	55.1–106.9	0.52–1.37	1.27–2.11	0.244–0.33	0.19–0.34
14.2	83.3–105.9	0.93–2.88	0.94–1.82	0.318–0.332	0.20–0.36
16	53.4–106	0.77–2.91	1.05–1.59	0.25–0.355	0.16–0.41
18	51.3–101.1	0.78–1.34	0.81–1.26	0.269–0.325	0.19–0.37

The velocity of a bubble (or a plug) was measured by the use of a Boscar motion analyzer from the developed films.

The instrumentation of the test tube is described elsewhere [7]. It will be sufficient to mention here that outlet temperature and pressure and mass flow on the water–steam side were measured with pre-calibrated instruments, and collected on an on-line data acquisition system and processed by a computer, Hewlett–Packard 2216B.

The water–steam side outlet temperature was measured with an inconel sheathed, chromel–alumel thermocouple of 0.5 mm O.D. The maximum error in determining this temperature was 1.2 K.

The water–steam side outlet pressure was measured with a dead-weight balance manometer, which had an error of 0.03 MN/m².

The water–steam side mass flow was measured with a turbine flowmeter, which had errors less than 1% for mass velocities higher than 96 kg/m² s in accordance with the manufacturer's data. Below the aforesaid mass velocity the turbine flowmeter was calibrated with an estimated accuracy of 10%.

ANALYSIS OF DATA

Plug flow

In the plug-flow regime, bubbles assumed either the shape of a plug or of a spherical cap, and $D/d > 0.6$, i.e. the magnitude of the equivalent diameter of a plug was in the same order of magnitude as the hydraulic diameter of the sapphire channel. In order to determine the equivalent diameter of a plug, the plug was considered to be elliptically shaped, and the minor and major axes of the plug were measured with a Boscar motion analyzer. The arithmetic mean of the aforesaid axes was taken as the equivalent diameter.

In the plug-flow regime, a few plugs (or even sometimes a single plug) and several comparatively very small bubbles in a liquid continuum were visible on the developed films. The velocity of every plug and bubble appearing on the film was measured at several axial positions (between 23 and 43 positions). The number of velocities measured varied between 79 and 145 for each test run. The reason why the velocity of a plug of a bubble was measured at several axial positions was to determine the time-averaged value of this velocity. In order to determine the weighted mean velocity of the vapour phase (or velocity of the centre

of gravity of the vapour phase) the following equation was used:

$$U \sum_{m=1}^m \frac{\pi}{6} \rho_v D_m^3 = \frac{\pi}{6} \rho_v \left(\frac{D_1^3}{n} \sum_{n=1}^n \bar{V}_n + \frac{D_2^3}{n} \sum_{n=1}^n V_n + \dots + \frac{D_m^3}{n} \sum_{n=1}^n V_n \right). \quad (16)$$

Periodic variation of the volume of a plug (or a bubble) was observed during the rise of the plug (or bubble). This cyclic variation of the volume became negligible at pressures higher than 14.2 MN/m². During the rise, a plug (or a bubble) rotated slowly and irregularly.

Bubble flow-regime

In the bubble-flow regime, the equivalent bubble diameter varied between 0.81 and 3.87 mm and the bubble shape was ellipsoid. The number of bubbles on the developed films was between 1 and 20.

The weighted mean velocity of the vapour phase in this flow regime was determined by a statistical method from the measured velocities of a sufficient number of bubbles taken randomly from the bubble population. The sample size varied between all the bubbles in the population and one-third of all the bubbles in the population. The velocity and minor and major axes of each bubble in the sample were measured at several axial positions (i.e. between 15 and 72 positions). The number of velocities measured varied between 37 and 292 for each test run. The equivalent bubble diameter was found by averaging the measured major and minor axes of a bubble.

The weighted mean velocity of the vapour phase is determined with the formula below:

$$U \sum_{k=1}^k \frac{\pi}{6} \rho_v D_k^3 = \frac{\pi}{6} \rho_v \left[\frac{D_1^3}{n} \sum_{n=1}^n V_n + \frac{D_2^3}{n} \sum_{n=1}^n V_n + \dots + \frac{D_k^3}{n} \sum_{n=1}^n V_n \right]. \quad (17)$$

Determination of the steam quality

In order to determine J [see equation (2)], the steam quality has to be known. During all the test runs, the steam quality was very low. The evaluation of this from a heat balance, therefore, may involve a considerable error. For this reason, the steam quality was de-

terminated by solving the following fundamental identities, which hold for any two-phase flow

$$Q_v = UA_p = XGA/\rho_v \quad (18)$$

$$\bar{\alpha} = A_v/(A_L + A_v) = A_v/A, \quad (19)$$

as given below:

$$X = \frac{\bar{\alpha}\rho_v U}{G} \quad (20)$$

$\bar{\alpha}$, the void fraction in equation (20), was determined with the following equation

$$\bar{\alpha} = \frac{\pi}{6} \sum_{i=1}^m D_i^3/R. \quad (21)$$

First the data were compared with the preliminary correlation of the author [i.e. equation (14)] and with the well-known correlation of Peebles and Garber [4] used by Zuber *et al.* [1, 5–6] to predict the drift velocity for the bubble flow regime [i.e. equation (12)]. As can be seen from Fig. 1, the agreement of the aforesaid correlations with the data is far from satisfactory. Equation (12) has in fact been presented by Peebles and Garber [4] as the terminal rising velocity of a gas bubble in a stagnant liquid. These investigators have also given three other correlations in their paper for the terminal rising velocity as a function of the bubble diameter and properties of the gas and the liquid. These correlations did not fit the data well either.

Data for drift velocities were correlated with the following dimensionless equation

$$16.1 \left[\frac{(\rho_L - \rho_v)g\mu_L}{\rho_L^2 V_d^3} \right]^{1/3} = 1, \quad (22)$$

as shown in Fig. 2. The reason why the few data do not fit the correlation well is probably due to errors in measuring mass velocities below 96 kg/m² s.

It follows from Figs. 1 and 2 that the drift velocity does not significantly vary with pressure.

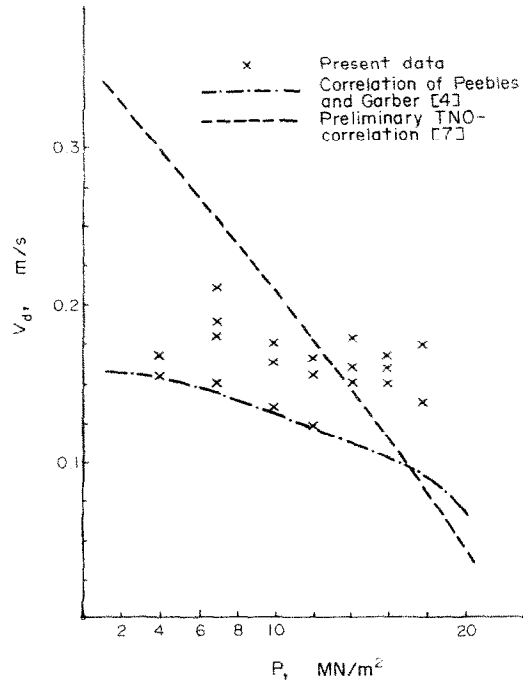


FIG. 1. Comparison of the data for the drift velocity with different correlations.

DETERMINATION OF VOID FRACTION

By the use of equations (5), (18) and (19), equation (15) can be modified to determine straightforwardly void fraction in the bubble- and plug-flow regimes for both low and high mass velocities

$$U/\bar{J} = \beta/\bar{\alpha} = 1 + 16.1[(\rho_L - \rho_v)g\mu_L/\rho_L^2]^{1/3}/\bar{J}. \quad (23)$$

Equation (23) has been compared in Fig. 3 with the present data and with data of the author for the weighted mean velocity of the vapour phase in bubble and plug flow [7]. The operating conditions for these data are summarized in Table 2. The agreement of equation (23) with the data is quite good.

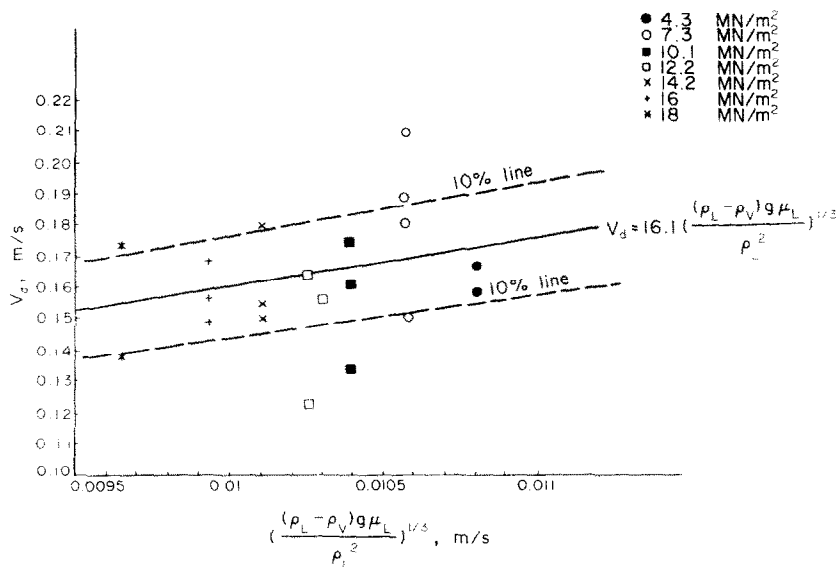


FIG. 2. Correlation of the data for the drift velocity.

Table 2. Conditions for void fraction experiments of various investigators

P (MN/m ²)	Number of data	Geometry	d (mm)	Heat flux (MW/m ²)	G (kg/m ² s)	X (%)	$\bar{\alpha}$ (%)	Reference
3–5	75	circular tube	9.16	adiabatic	388–3504	0–80	0–99	8
13.8	54	rectangular channel	4.74	0.32–1.58	895–1153	10–37	42–85	9
2–6.9	75	circular tube and annulus	7.7–10.2	adiabatic	400–3400	10–88	58–99	10
2–9.8	11	circular tubes	15.7–34.3	0.014–2	400–1700	10–60	49–99	10
1–5	365	annulus	13	0.60–1.22	127–1368	5–21.9	55–87	11
4.1–15.9	42	circular tube	8	0.10–0.50	1869–2383	0–2.9	$U = 2.8–4.8$ m/s	7

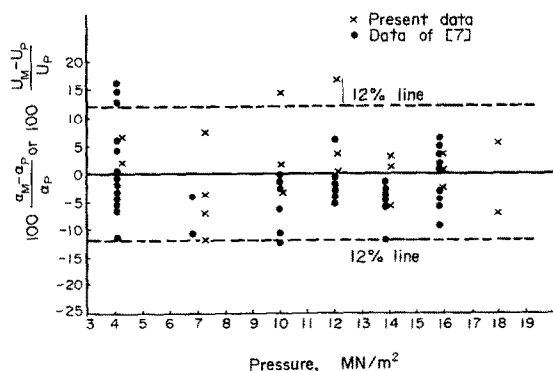


FIG. 3. Verification of equation (23).

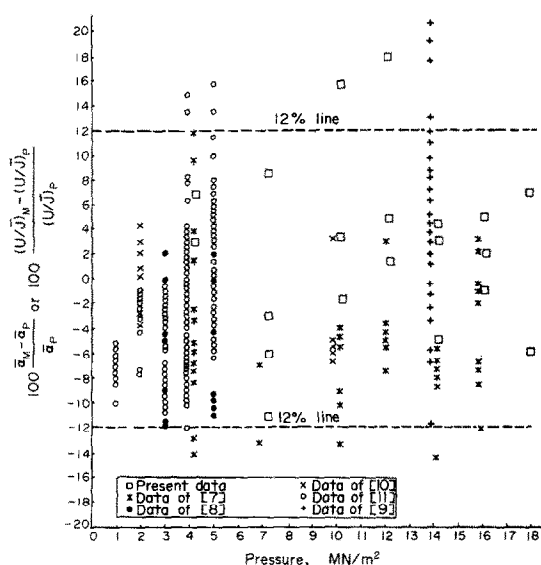


FIG. 4. Comparison of the void fraction data with equation (24).

Equation (23) has also been compared with the data of various investigators obtained for a wide range of operating conditions for the adiabatic and diabatic flow of steam–water mixtures in different types of channels [8–11]. In this comparison flow regimes are not considered. The number of data considered was 580. Not all the data from [9–11] could be considered. Only the data for comparatively high steam qualities, as indicated in Table 2, were studied, since for subcooled nucleate flow boiling, in which steam qualities are low, a simple heat balance does not give the steam quality as a result of the thermal non-

equilibrium existing between the phases. With the exception of the low mass velocity data of [11] taken in an annulus for $P = 1–5$ MN/m² and $G \approx 130$ kg/m² s, the agreement of the data with the equation (23) was satisfactory.

In order to correlate all the aforesaid data, equation (23) was modified as follows

$$\beta/\bar{\alpha} = 1.03 + V_d/\bar{J}. \quad (24)$$

V_d in equation (24) is given by equation (22) for circular tubes and rectangular channels, and with the following equation for annuli

$$V_d = 40.25[(\rho_L - \rho_v)\mu_L g/\rho_L^2]^{1/3}. \quad (25)$$

Results of the comparison of equation (24) with the data are shown in Fig. 4. Since the number of data considered was large, i.e. 642, not all the data could be given in the figure. The data shown in the figure have been selected in such a way that the range of maximum error in predicting void fraction can be seen. Equation (24) correlates all the data within 12% accuracy with the exception of 15 data, as can be deduced from the figure. The RMS error for correlating the data is 6%.

For the 449 data considered $V_d/\bar{J} \ll 1$. It follows from equation (24) that the value of C , the distribution parameter is practically equal to one, i.e. radial-void and -volume flux density distributions in small channels are not of importance to predict void fraction. The above statement does not imply that the radial-void and -volume flux density distributions do not exist in a small-diameter channel. The same conclusion is drawn also in [7]. In [7] the drift velocity was evaluated by equation (14) and the data summarized in Table 2, with the exception of low-mass velocity data of [11], were used.

The operating conditions and geometry for which equation (24) has been verified, are summarized below.

Geometry: vertical tubes, vertical annuli and vertical rectangular channels

P , 1–18 MN/m²;

$\bar{\alpha}$, 0.08–99%;

d , 0.0047–0.0343 m;

G , 51–3504 kg/m² s;

q , adiabatic (without heat addition) and 0.01–2.0 MW/m².

Throughout this study, properties of water and steam were evaluated from [12].

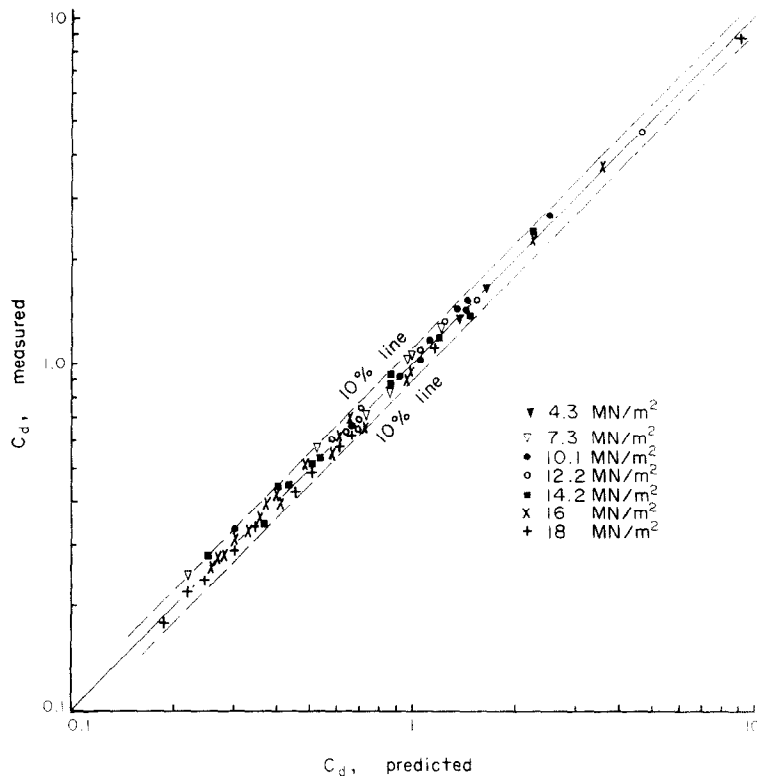


FIG. 5. Comparison of the data for drag coefficient with equation (28).

DRAW COEFFICIENT

The drag coefficient is the ratio of buoyancy to drag forces acting on a bubble (or a plug), and is given by the following equation for the steady-motion of a bubble (or a plug):

$$C_d = \frac{4}{3} \frac{\rho_L - \rho_v}{\rho_L} \frac{gD}{u^2} \quad (26)$$

where u is the difference between the time-averaged bubble velocity and local liquid velocity. In order to determine C_d for bubble flow, the local liquid velocity was taken equal to the average liquid velocity based on total mass flow and the cross sectional area of the sapphire channel for the following two reasons: Firstly, for the bubble-flow region the measured void fraction was very low, i.e. between 0.08% and 4.55% (see Table 1). Secondly, owing to the transition piece between the sapphire channel and the test tube, the velocity profile in the sapphire channel could be assumed to be uniform except in the boundary layer near the channel wall.

For plug flow, the local liquid velocity was taken equal to the average liquid velocity based on total mass flow and the cross sectional area of the sapphire channel. The bubble (or the plug) velocity was determined with the equation below

$$\bar{V} = \frac{1}{n} \sum_{i=1}^n V_i \quad (27)$$

Data for the drag coefficient were correlated with the following equation:

$$C_d = \frac{\exp(18.967 + 2.74a - 28.35a^2 + 48.75a^3 - 32.82a^4)}{Re^2} \quad (28)$$

where

$$a = (1 - D/d) \quad (29)$$

$$Re = \frac{u \rho_L D}{\mu_L} \quad (30)$$

The range of data is given in Table 1. The bubble (or the plug) Reynolds number varied between 372 and 11 256. The number of data was 77. The accuracy of equation (28) is 10%, as shown in Fig. 5, and the RMS error in correlating the data was 4.4%.

FLOW PATTERN INSTABILITIES

During the analysis of the developed films, a flow pattern instability was observed. For pressures lower than 16 MN/m², the flow regime varied from bubble flow to plug flow with a frequency between 10 and 50 Hz. During the measurement of void fraction in a 26.7 m and in a 40.1 m long sodium heated helical coil of 0.018 m I.D., a similar type of instability was also observed for $P = 4\text{--}8.1$ MN/m² and $G = 429\text{--}1518$ kg/m²s [13]. Jeclic and Yang [14] detected analogous instabilities in an electrically heated vertical tube.

In the literature the cause of this type of instability is related to the variation of the pressure drop in the bubble-slug flow and in the annular flow regimes [15].

Since the present test tube is very long, the variation of the pressure drop in different flow regimes can not be the cause of the observed instabilities. Moreover, no annular flow was observed during these instabilities.

At present the cause of the observed instabilities is speculated to be the suppression of bubble growth. Bubbles grow at the heated wall, depart from the wall, coalesce, and form a plug. The volume of the plug varies periodically and the plug rotates irregularly and, therefore, destroys the superheated liquid layer on the heated wall. The destruction of this layer delays the growth of bubbles. For the time interval in which enough bubbles are produced to form a plug, the bubble flow regime exists in the test tube and the plug flow regime thereafter.

The other type of instabilities relevant to a long steam generator tube is discussed in detail in [15–17].

Acknowledgements—This study is a government-sponsored work carried out at TNO. The author wishes to thank Messrs. K. A. Warschauer, A. R. Braun and M. L. G. van Gassel for their encouragement during the preparation of this work. Mr. C. van Huffelen has analysed the films.

REFERENCES

1. N. Zuber and J. A. Findlay, Average volumetric concentration in two-phase flow systems, *J. Heat Transfer* **87**, 453–468 (1965).
2. N. M. Aybers, Transport of gas bubbles through a stagnant liquid and turbulent liquid stream, Paper presented at Nato Advanced Study Institute on Two-Phase Flows and Heat Transfer, Istanbul, Turkey (August 16–27, 1976).
3. G. B. Wallis, *One-dimensional Two-Phase Flow*. McGraw-Hill, New York (1969).
4. F. N. Peebles and H. J. Garber, Studies on the motion of gas bubbles in liquids, *Chem. Engng Prog.* **49**, 88–97 (1953).
5. N. Zuber, F. W. Staub and G. Bijwaard, Vapor void fraction in subcooled boiling and in saturated boiling systems, in *Proceedings of the Third International Heat Transfer Conference*, 7–12 August, 1966, Chicago, Illinois, Vol. 5, pp. 24–38. A.I.Ch.E., New York (1966).
6. F. W. Staub and N. Zuber, Void fraction profiles, flow mechanisms and heat transfer coefficients for Refrigerant 22 evaporating in a vertical tube, in *ASHRAE Transactions*, Vol. 72, Part I, pp. 130–146 (1966). ASHRAE, New York.
7. H. C. Ünal, Void fraction and incipient point of boiling during the subcooled nucleate flow boiling of water, *Int. J. Heat Mass Transfer* **20**, 409–419 (1977).
8. G. Agostini, A. Era and A. Premoli, Density measurements of steam-water mixtures flowing in a tubular channel under adiabatic and heated conditions, *Energia Nucl., Milano* **18**, 295–310 (1971).
9. R. A. Egen, D. A. Dingee and J. W. Chastain, Vapor formation and behaviour in boiling heat transfer, Battelle Memorial Institute Report, 1163 (1957).
10. Z. L. Miropolskiy, R. I. Shneyerova and A. I. Karamysheva, Vapor void fraction in steam fluid mixtures flowing in heated and unheated channels, Preprints of papers presented at the Fourth International Heat Transfer Conference, Paris Versailles 1970, in *Heat Transfer 1970*, edited by U. Grigull and E. Hahne, Vol. 5, Paper No. B4.7. Verein Deutscher Ingenieure, Dusseldorf (1970).
11. S. Z. Rouhani, Void measurements in the regions of subcooled and low-quality boiling, AE-239, Aktiebolaget Atomenergi, Stockholm, Sweden (1966).
12. The American Society of Mechanical Engineers, 1967 *ASME Steam Tables*. ASME, New York (1967).
13. H. C. Ünal, Determination of void fraction, incipient point of boiling and initial point of net vapour generation in sodium heated helically coiled steam generator tubes, *J. Heat Transfer*, to be published.
14. F. A. Jeclic and K. T. Yang, The incipience of flow oscillations in forced-flow subcooled boiling, NASA TM X-52081 (1965).
15. J. A. Bouré, A. E. Bergles and L. S. Tong, Review of two-phase flow instability, *Nucl. Engng Des.* **25**, 165–192 (1973).
16. H. C. Ünal, An investigation of the inception conditions of dynamic instabilities in sodium heated steam generator pipes, Paper presented at Nato Advanced Study Institute on Two-Phase Flows and Heat Transfer, Istanbul, Turkey (August 16–27, 1976).
17. H. C. Ünal, M. L. G. van Gassel and P. W. P. H. Ludwig, Dynamic instabilities in tubes of a large capacity, straight-tube, once-through sodium heated steam generator, *Int. J. Heat Mass Transfer*, to be published.

DETERMINATION DE LA VITESSE D'ENTRAÎNEMENT ET DE LA FRACTION DE VIDE DANS LES REGIMES D'ÉCOULEMENT A BULLES ET A BOUCHONS POUR L'ÉCOULEMENT DE L'EAU EN EBULLITION A DES PRESSIONS ÉLEVÉES

Résumé—On a déterminé la vitesse d'entraînement à des pressions élevées au moyen de la photographie ultra-rapide pour les régimes d'écoulement à bulles et à bouchons dans un canal de générateur de vapeur chauffé au sodium, d'une longueur de 10 m et d'un diamètre intérieur de 0,008 m. On a réalisé les expériences sous les conditions suivantes: pression: 4,3–18 MN/m²; vitesse massique: 51–107 kg/m²s; sous-refroidissement à la sortie: 0–1,3 K; fraction de vide: 0,0008–0,26. Les données ont été corrélées à l'aide d'une équation non dimensionnelle. Pour les conditions opératoires considérées, la vitesse d'entraînement n'a pas changé sensiblement. Pour la détermination de la fraction de vide, avec un large domaine de conditions, dans des canaux circulaires de faible diamètre, des canaux annulaires et rectangulaires, la corrélation donnée par l'auteur a été modifiée légèrement. La corrélation s'applique à la fois à des hautes et à des basses vitesses massiques. Le coefficient de traînée pour le mouvement d'une bulle (ou d'un bouchon) dans un courant d'eau turbulent est une fonction du nombre de Reynolds de la bulle (ou du bouchon) et de la géométrie. Pendant les expériences, pour le domaine de pression de 4,3 MN/m² à 14,2 MN/m², la configuration d'écoulement dans le canal expérimental a changé périodiquement de l'écoulement à bulles à l'écoulement à bouchons. La fréquence des instabilités observées a varié entre 10 et 50 Hz. On prévoit que la cause de ce type d'instabilité est la suppression de la croissance des bulles.

BESTIMMUNG DER DRIFTGESCHWINDIGKEIT UND DES DAMPFGEHALTS
VON BLASEN- UND PFROPFENSTRÖMUNG BEIM SIEDEVORGANG VON
STRÖMENDEM WASSER BEI HÖHEREN DRÜCKEN

Zusammenfassung—Die Driftgeschwindigkeit ist mittels ultraschneller Fotografie bei höheren Drücken für Blasen- und Pfropfenströmung in einem 10 m langen natriumbeheizten Dampferzeugerrohr mit 0,008 m Innendurchmesser gemessen worden. Die Betriebsbedingungen für die Experimente waren: Druck 4,3–18 MN/m²; Massenfluß 51–107 kg/m² s; Unterkühlung am Austritt: 0–1,3 K; Dampfgehalt 0,0008–0,26. Die Daten sind mittels einer dimensionslosen Gleichung korreliert worden. Für die betrachteten Betriebsbedingungen ändert sich die Driftgeschwindigkeit nicht wesentlich. Um den Dampfgehalt für einen weiten Bedingungsbereich in kreisrunden Rohren von kleinem Durchmesser, in Spalten und rechtwinkligen Kanälen zu bestimmen, ist die Korrelation vom Verfasser leicht geändert worden. Die Korrelation ist sowohl für hohe als auch für niedrige Massenflüsse gültig. Der Strömungswiderstandskoeffizient für die Bewegung einer Blase (oder eines Pfropfens) in einem turbulenten Wasserstrom konnte als Funktion der Reynolds Zahl der Blase (oder des Pfropfens) und der Geometrie dargestellt werden. Während der Experimente im Druckbereich von 4,3 MN/m² bis 14,2 MN/m² änderte sich die Strömungsform im Testrohr periodisch von Blasenströmung in Pfropfenströmung. Die Frequenz der wahrgenommenen Instabilitäten variierte zwischen 10 und 50 Hz. Als Ursache dieser Art Instabilität ist anzunehmen, daß das Wachsen der Blase unterdrückt wird.

ОПРЕДЕЛЕНИЕ СКОРОСТИ ДРЕЙФА И ИСТИННОГО ОБЪЕМНОГО
ПАРОСОДЕРЖАНИЯ ДЛЯ ПУЗЫРЬКОВЫХ И СНАРЯДНЫХ РЕЖИМОВ
ТЕЧЕНИЯ ПРИ КИПЕНИИ В ПОТОКЕ ВОДЫ ПРИ ПОВЫШЕННЫХ ДАВЛЕНИЯХ

Аннотация — Скорость дрейфа при повышенном давлении измерялась с помощью высокоскоростной съемки для режимов пузырькового и снарядного течения в парогенераторной трубке длиной 10 м и диаметром 0,008 м, нагреваемой натрием. Опыты проводились при давлении 4,3–18 МН/м², массовом расходе 51–107 кг/м² сек, недогреве на выходе 0–1,3 К и коэффициенте истинного объемного паросодержания 0,0008–0,26. Данные обобщались с помощью безразмерного уравнения. В рассматриваемых рабочих условиях значительного изменения в скорости дрейфа не наблюдалось. Для определения истинного объемного паросодержания в широком диапазоне условий, имеющих место в трубах небольшого диаметра, кольцевых и прямоугольных каналах, предложенная автором критериальная зависимость была несколько видоизменена. Эта зависимость справедлива как при высоких, так и при малых массовых расходах. Показано, что коэффициент сопротивления для пузырька (или снаряда) в турбулентном потоке водяного пара является функцией числа Рейнольдса для пузырькового (или снарядного) режима течения и геометрии канала. В процессе эксперимента (в диапазоне давлений от 4,3 МН/м² до 14,2 МН/м²) картина течения в трубке периодически изменялась от пузырькового до снарядного режима. Частота периодов составляла от 10 до 50 гц. Предполагается, что причиной такого типа неустойчивости является подавление роста пузырьков.